Journal of Achievements in Materials and Manufacturing Engineering
VOLUME 22
ISSUE 1
May
2007

Simulation of induction heating process with radiative heat exchange

A. Kachel, R. Przyłucki*
Department of Electrotechnology, Faculty of Metallurgy and Material Science, Silesian University of Technology, ul. Krasińskiego 8, 40-019 Katowice, Poland
* Corresponding author: E-mail address: roman.przylucki@polsl.pl

Received 14.03.2007; published in revised form 01.05.2007

Analysis and modelling

ABSTRACT

Purpose: Numerical modelling of induction heating process is a complex issue. It needs analysis of coupled electromagnetic and thermal fields. Calculation models for electromagnetic field analysis as well as thermal field analysis need simplifications. In case of thermal field calculations, correct modelling of radiative heat exchange between the heated charge and inductor's thermal insulation is essential. Most commercial calculation programs enabling coupled analysis of electromagnetic and thermal fields do not allow taking into consideration radiative heat exchange between calculation model components, which limits thermal calculations only to the charge area. The paper presents a supplementation of the program Flux 2D with radiative heat exchange procedures.
Design/methodology/approach: Commercial program Flux 2D designed for coupled electromagnetic and thermal calculation (based on finite element method) was supplemented with authors program for radiative heat exchange based on numerical integration of classic equations.
Findings: Supplementation EM-T calculations with radiative heat exchange between charge and inductor enables to calculate thermal insulation parameters and increase precision of modelling.
Research limitations/implications: Procedures for radiative heat exchange enables calculation of two surfaces (flat or cylindrical) with finite dimensions. The surfaces can be displaced relative to each other (charge shorter or longer than thermal insulation of inductor). Material of surfaces is modelled as: flat, diffuse, radiant surfaces absorb energy evenly in the whole spectrum (grey bodies). The whole system is modelled as in a steady thermal state (quasi-steady).
Originality/value: Authors program extends Flux 2D features with a possibility for calculating radiative heat transfer. The application of radiative process is possible between all components of the studied model, not only for the boundary conditions.
Keywords: Numerical techniques; Induction heating

1. Introduction

The article discusses the implementation of radiative heat exchange into the program Flux 2D. It extends features of that commercial program, and opens the way to calculation of more realistic model of induction heating process. Flux 2D enables calculations of coupled electromagnetic-thermal fields, but has several limitations. One of them is that it is impossible to calculate radiative heat exchange between components of the model. It is possible to calculate thermal emission from the part of model to outside space only. Such way of calculation causes that model for thermal calculation of induction heating is usually limited to the heating charge only. The features of extended package Flux 2D are presented on the example of three variants of calculations. Variants differed in geometrical dimensions and in the way how the heat exchange was modelled. During the experiment temperature distribution in the model was controlled.

2. Calculation model

For the experiment the system whose geometry is shown in Figure 1 was chosen. It is a model of induction heater for flat charges. It

consists of charge (non-ferromagnetic steel), thermal insulation and copper inductor. Main dimensions of the model system are as follows: charge width w_c = 20 mm, height of charge h_c = 100 mm, air gap between charge and thermal insulation a_g = 7 mm, thermal insulation thickness w_t = 5 mm. Inductor coil profile has width w_w = 10 mm, height h_w = 12 mm and thickness of profile is t_w = 2 mm.

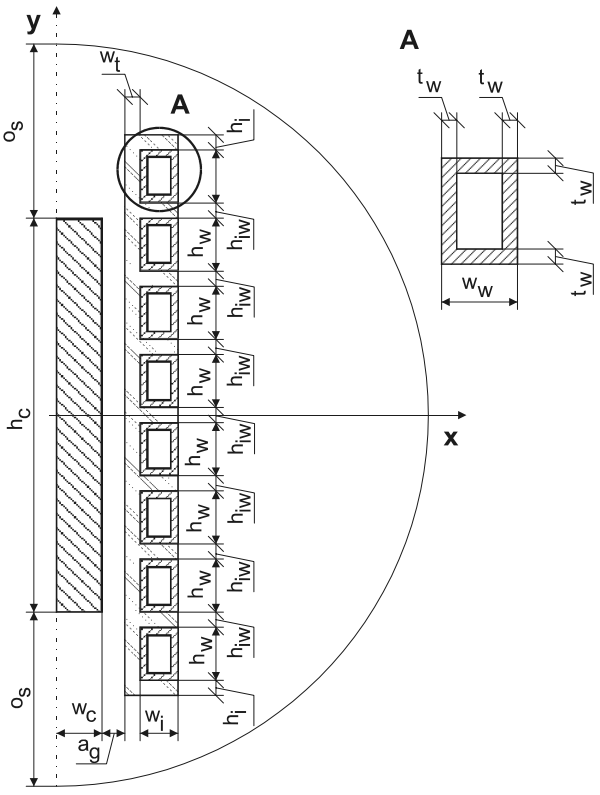

Fig. 1. Calculation model geometry

Electromagnetic calculations for all variants were performed for the same calculation model showed in Figure 1. Equations (1) to (3) [1-6] with proper boundary conditions (4) were used. Calculation areas are: Ω_1 – charge, Ω_2 – thermal insulation, Ω_3 - inductor, Ω_4 – water, Ω_5 – air. Boundary conditions are applied in places showed in Figure 2.

$$\Omega_1: \quad \nabla\times\nabla\times\underline{A} + j\omega\gamma\mu\underline{A} = 0 \tag{1}$$

$$\Omega_3: \quad \nabla\times\nabla\times\underline{A} + j\omega\gamma\mu\underline{A} = \mu J_s \tag{2}$$

$$\Omega_2,\Omega_4,\Omega_5: \quad \nabla\times\nabla\times\underline{A} = 0 \tag{3}$$

$$\overline{ae}, \overline{ef}, \overline{fd}, \overline{da}: \quad \underline{A} = 0 \tag{4}$$

where: A – (Vs/m) magnetic vector potential, J_s – (A/m^2) source current density, ω – (rad/s) angular frequency, μ – (Vs/(Am)) magnetic permeability.

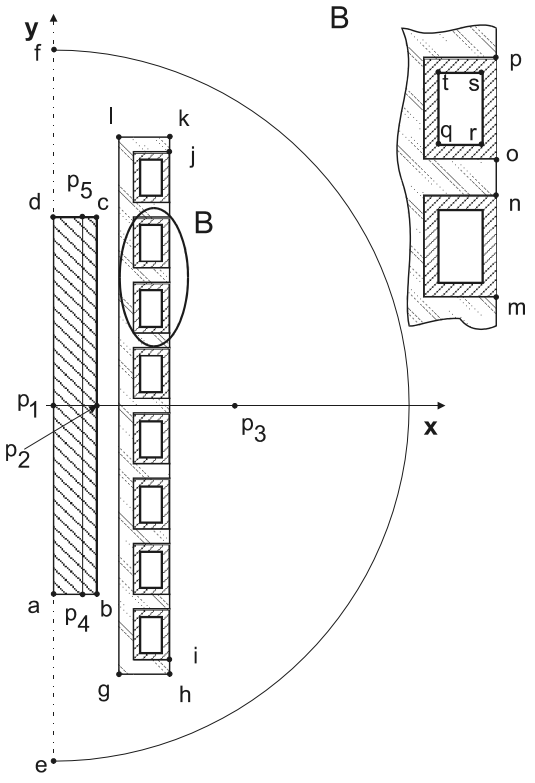

Fig. 2. Boundary conditions specification

Inductor was powered by AC current source of I = 3000 A and frequency f = 1000 Hz. Thermal calculations were performed in three different ways. In the first variant (v1) of calculations thermal model was reduced to charge area only. In the second one (v2) full geometry was considered. In the third variant (v3) radiative heat exchange was included. Thermal calculations were based on equations (5), (6) [1-6].

$$\Omega_1,\Omega_3: \quad \rho c\frac{\partial T}{\partial t} + \nabla\cdot(-\lambda\nabla T) = q \tag{5}$$

$$\Omega_2,\Omega_4,\Omega_5,: \quad \rho c\frac{\partial T}{\partial t} + \nabla\cdot(-\lambda\nabla T) = 0 \tag{6}$$

where: ρ – (kg/m^3) density, c – (J/(kg K)) specific heat capacity, T – (K) temperature, t – (s) time, λ – (W/ (mK)) thermal conductivity, q – (W/m^3) power density per volume.

Boundary conditions described by equations (7) to (8) are identical for all calculation variants.

$$\overline{ad}: \quad -\lambda\frac{dT}{dn} = 0 \tag{7}$$

$$\overline{ab},\overline{cd}: \quad -\lambda\frac{dT}{dn} = \alpha(T - T_a) + \varepsilon\sigma(T^4 - T_a^4); \quad \alpha = 10; \quad \varepsilon = 0.6; \quad T_a = 20 \tag{8}$$

For the second calculation variant following boundary conditions were applied (9) to (11).

$$\overline{bc}, \overline{gh}, \overline{hi}, \overline{jk}, \overline{kl}, \overline{lg}, \overline{mn}, \overline{no}, \overline{op}: \quad -\lambda \frac{dT}{dn} = \alpha (T - T_a) + \varepsilon\sigma (T^4 - T_a^4); \tag{9}$$

α = 10, Ta = 20, ε = 0.6 for edge $\overline{bc}$; ε = 0.4 for edge $\overline{mn}, \overline{op}$; ε = 0.5 for edge $\overline{gh}, \overline{hi}, \overline{jk}, \overline{kl}, \overline{lg}, \overline{no}$.

$$\overline{ae}, \overline{fd}: \quad -\lambda \frac{dT}{dn} = 0 \tag{10}$$

$$\overline{ef}, \overline{qr}, \overline{rs}, \overline{st}, \overline{tq}, : \quad T = 20 \tag{11}$$

For the third calculation variant boundary conditions are the same as in the second case with following changes:

$$\overline{bc}, \overline{lg}: \quad -\lambda \frac{dT}{dn} = \alpha (T - T_a); \quad \alpha = 10; \quad T_a = 20 \tag{12}$$

More over the radiative heat exchange was included between edges: $\overline{bc}, \overline{lg}$.

3. Thermal radiation model

Radiative heat exchange in the flat charge - heater heating system takes place between two surfaces with finite dimensions. The surfaces can be displaced relative to each other (charge shorter or longer than thermal insulation of inductor). Most often surfaces are parallel. Typical configuration of the studied system model is presented in Figure 3.

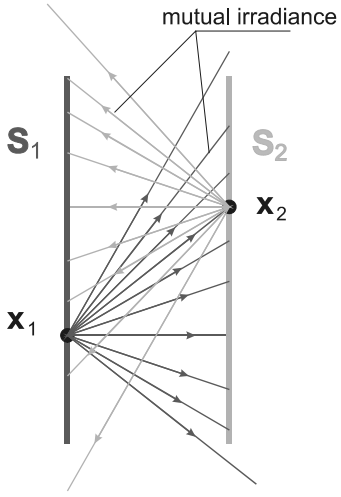

Fig. 3. Radiant surface system

To include the radiative heat transfer in the considered model the following simplifications were assumed: the whole system is in a steady thermal state (quasi-steady), radiant surfaces are flat, both primary and reflected radiation are of Lambertian, diffuse type, radiant bodies absorb energy evenly in the whole spectrum.

By applying Lambert and Kirchhoff laws in a simple expression of radiative energy balance a system of integral equations (13), (14) is obtained [7-16]. Solution of the system of equations describes total radiant exitance emitted from the particular surfaces S_1 and S_2. The total radiant exitance for each surface determines resulting, effective radiation, being the sum of primary and reflected radiations. Equations (15) and (16) describe resulting irradiance and heat transfer by radiation, respectively. To solve the equations a numerical method was used [7-15].

$$U_1(\mathbf{x}_1) = a_1\sigma T_1^4 + (1 - a_1)\int_{S_2} k(\mathbf{x}_1, \mathbf{x}_2) U_2(\mathbf{x}_2)\, dS_2 \tag{13}$$

$$U_2(\mathbf{x}_2) = a_2\sigma T_2^4 + (1 - a_2)\int_{S_1} k(\mathbf{x}_2, \mathbf{x}_1) U_1(\mathbf{x}_1)\, dS_1 \tag{14}$$

$$I_i(\mathbf{x}_i) = \frac{U_i(\mathbf{x}_i) - a_i\sigma T_i^4}{1 - a_i} \tag{15}$$

$$Q_i(\mathbf{x}_i) = a_i\left[I_i(\mathbf{x}_i) - \sigma T_i^4\right] \tag{16}$$

where: U – (W/m^2) total radiant exitance, a - absorption coefficient (a ≡ ε), σ – (W/(m^2 K^4) Stefan – Boltzman coefficient, $k(\mathbf{x}_i,\mathbf{x}_j)$ - optical coupling function (integral kernels, i ≠ j), I_i – (W/m^2) irradiance, Q_i – (W/m^2) radiative heat exchange, i,j = 1,2.

4. Results

During the experiment induction heating of steel charge for 40 seconds was simulated. Temperature distribution along paths pa_1 (segment $\overline{p_1p_2}$), pa_2 (segment $\overline{p_1p_3}$) and pa_3 (segment $\overline{p_4p_5}$) was studied.

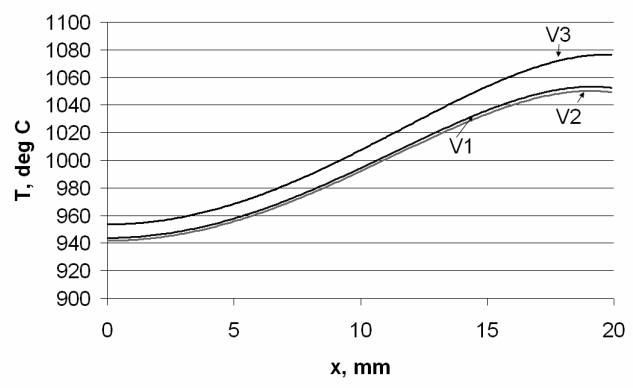

Fig. 4. Temperature distribution along path pa_1 after 40 s

For all analyzed cases the most significant temperature differences appear at the end of heating (after 40 s.). Temperature distribution on path pa_1 is showed in Figure 4. Maximum temperature difference is about 27 °C. Along path pa_2 temperature differences are more essential, and reaching 677 °C (Figure 5). It appears in air gap and thermal insulation area. Figure 6 show temperature distribution along pa_3 (1 mm under surface of heated charge). Temperature differences do not exceed 25 °C.

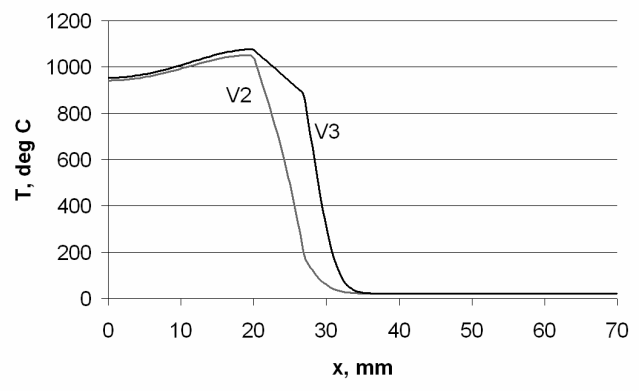

Fig. 5. Temperature distribution along path pa_2 after 40 s

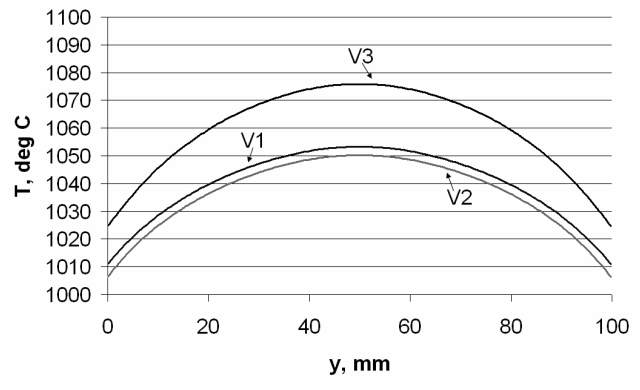

Fig. 6. Temperature distribution along path pa_3 after 40 s

5. Conclusions

Inclusion of radiative heat transfer between charge and thermal insulation makes the calculations of induction heating more precise. For the studied case taking for consideration radiative heat exchange changes maximally temperature difference value in charge by 27 °C (between variants v2 and v3), but in air gap and thermal insulation temperature differences reach 677 °C. Supplementation Flux 2D with authors procedures for radiative heat transfer enables thermal calculations of inducting heating systems consists with charge, air gap, thermal insulation, inductor and other parts. It opens the way to proper design of thermal insulation thickness and in consequence to more optimal construction of the induction heater.

Acknowledgements

This work was sponsored by Ministry of Scientific Research and Information Technology as a grant no. 3T08B06428.

References

[1] Cedrat, Flux 2D User's Guide, 2006.
[2] H. Kawaguchi, M. Enokizono, T. Todaka, Thermal and magnetic field analysis of induction heating problems, Journal of Materials Processing Technology 161 (2005) 193-198.
[3] H.K. Jung, The induction heating process of semi-solid aluminium alloys for thixoforming and their microstructure evaluation, Journal of Materials Processing Technology 105 (2000) 176-190.
[4] D.C. Ko, G.S. Min, B.M. Kim, J.C. Choi, Finite element analysis for the semi-solid state forming of aluminium alloy considering induction heating, Journal of Materials Processing Technology 100 (2000) 95-104.
[5] Z. Hu, J.Q. Li, Computer simulation of pipe-bending processes with small bending radius using local induction heating, Journal of Materials Processing Technology 91 (1999) 75-79.
[6] K.L. Schlemmer, F.H. Osman, Differential heating forming of solid and bi-metallic hollow parts, Journal of Materials Processing Technology 162-163, 2005, 564-569.
[7] R. Siegel, J.R. Howell, Thermal Radiation Heat Transfer, Mc-Graw Hill Book Co., N. York, 1972.
[8] M.F. Cohen, D.P. Greenberg, The hemi-cube: a radiosity solution for complex environment, Computer Graphics, 1985.
[9] J. Kajiya, The Rendering Equations, Computer Graphics 20, 1986.
[10] P. Dutré, Global Illumination Compendium, Cornell University, 2001.
[11] M.F. Modest, Radiative Heat Transfer. Second Edition, Academic Press Amsterdam, Boston – London - N. York - Sydney, 2003.
[12] A. Kachel, R. Przyłucki, Two dimensional model of radiative heat exchange in heater - flat charge system, Proceedings of the International Conference on Research in Electrotechnology and Applied Informatics, Katowice, 2005, 153-158.
[13] K. Domke, Modelling of radiative heat transfer using computer graphics programs, Proceedings of the International Conference on Research in Electrotechnology and Applied Informatics, Katowice, 2005, 79-84.
[14] P. Furmanski, J. Banaszek, Some new computational models of radiative heat transfer in participating media, Progress in Computational Fluid Dynamics 5 (2005) 222-229.
[15] W.M. Gao, L.X. Kong, P.D. Hodgson, Numerical simulation of heat and mass transfer in fluidised bed heat treatment furnaces, Journal of Materials Processing Technology 125-126 (2002) 170-178.
[16] H.P. Zeng, J.C. Fang, W.J. Xu, Z.Y. Zhao, L. Wang, Thermo-mechanical modeling of a single splat solidification in plasma spraying, Journal of Achievements in Materials and Manufacturing Engineering 18 (2007) 327-330.